Fulvic acids from Amazonian anthropogenic soils: Insight into the molecular composition and copper binding properties using fluorescence techniques

João Vitor dos Santos, Lais Gomes Fregolente, Stéphane Mounier, Houssam Hajjoul, Odair Pastor Ferreira, Altair Benedito Moreira, Márcia Cristina Bisinoti

Fulvic acids from Amazonian anthropogenic soils: Insight into the molecular composition and copper binding properties using fluorescence techniques

João Vitor dos Santos[a,b], Laís Gomes Fregolente[a,c], Stéphane Mounier[b], Houssam Hajjoul[b], Odair Pastor Ferreira[c], Altair Benedito Moreira[a], Márcia Cristina Bisinoti[a*]

[a]Laboratório de Estudos em Ciências Ambientais, Departamento de Química e Ciências Ambientais, Instituto de Biociências, Letras e Ciências Exatas, Universidade Estadual Paulista "Júlio de Mesquita Filho," 15054-000, São José do Rio Preto, São Paulo, Brazil.

[b]Université de Toulon, Aix Marseille Univ., CNRS/INSU, IRD, MIO UM 110, Mediterranean Institute of Oceanography, CS 60584, 83041 – TOULON.

[c]Laboratório de Materiais Funcionais Avançados, Departamento de Física, Universidade Federal do Ceará, 60455-900, Fortaleza, Ceará, Brazil.

[*]Corresponding author

Name: Márcia Cristina Bisinoti

E-mail: marcia.bisinoti@unesp.br

Phone: +55 17 3221-2352

Address: Laboratório de Estudos em Ciências Ambientais, Departamento de Química e Ciências Ambientais, Instituto de Biociências, Letras e Ciências Exatas, Universidade Estadual Paulista "Júlio de Mesquita Filho", Rua Cristóvão Colombo, 2265, 15054-000, São José do Rio Preto, São Paulo State, Brazil.

Abstract

Fulvic acids (FA) are one of the components of humic substances and play an important role in the interaction with metallic species and, consequently, the bioavailability, distribution and toxicity of metals. However, only a few studies have investigated these FA properties in specific environment, such as anthropogenic soils. Therefore, knowledge about FA molecular composition as well as the FA-metal interaction is essential to predict their behavior in the soil. For this reason, the aim of this study was to investigate the molecular composition of FA extracted from two sites in an anthropogenic soil (*Terra Mulata*), from the Amazon region, as well as their interactions with Cu(II) ions as a model. Results from ^{13}C NMR, infrared and elemental analysis showed that these FA are composed mostly by alkyl structures and oxygen-functional groups, e.g., hydroxyl, carbonyl and carboxyl. The interaction with Cu(II) ions was evaluated by fluorescence quenching, in which the FA showed both high quantity of complexing sites per gram of carbon and good affinity to interact with the metal when compared with other soil FA. The results showed that the complexation capacity was highly correlated by the content of functional groups, while the binding affinity was largely influenced by structural factors. In addition, through the lifetime decay given by time-resolved fluorescence, it was concluded that static quenching took place in FA and Cu(II) interaction with the formation of a non-fluorescent ground-state complex. Therefore, this fraction of soil organic matter will fully participate in complexation reactions, thereby influencing the mobility and bioavailability of metal in soils. Hence, the importance of the study, and the role of FA in the environment, can be seen especially in the Amazon, which is one of the most important biomes in the world.

Keywords: *Terra Mulata* soils, humic substances, metal complexation, PARAFAC, lifetime

1. Introduction

The Amazon biome has worldwide importance (Coe et al., 2013) due to its extent, biodiversity, and acting as a large carbon reservoir (Batjes and Dijkshoorn, 1999). Amazonian anthropogenic soils, also called *Terra Mulata* (TM) soils are found in some Amazon regions. They are dark colored soils, with a high nutrient content and high fertility (dos Santos et al., 2020; Oliveira et al., 2018; Lucheta et al., 2017; Fraser et al., 2011; Cunha et al., 2009; Glaser et al., 2000), contrasting with other Amazonian soils which are highly acidic, with low fertility and cation exchange capacity (Soares et al., 2005). Their formation is still unclear, but researches have pointed out that, human activity in the pre-Columbian past has resulted in a large organic matter and nutrient accumulation over the years (Clement et al., 2015; Novotny et al., 2009). Therefore, such soils have been considered as a model for sustainable agriculture (dos Santos et al., 2020; Novotny et al., 2009).

The organic matter characteristics vary among soils (Baird and Cann, 2012), making the characterization and documentation of each TM site very important once the area of occurrence is restricted and limited, in order to know as much as possible about their characteristics and particularities (Novotny et al., 2009). Studies have shown that the organic matter from Amazonian anthropogenic soils is recalcitrant, due to the presence of carbon nanoparticles with graphite-like cores, in which their structures are very stable (Archanjo et al., 2014; Oliveira et al., 2018). This graphite-like structure prolongs the carbon residence time in the soil.

Humic substances (HS) are the main constituents of soil organic matter, and are formed from the remains of plant and animal degradation (Stevenson, 1994). According to its solubility in aqueous medium, HS is usually grouped in three fractions: humic acids (HA), fulvic acids (FA) and humin (HU). In the literature several studies are reported, with the most diverse purposes, involving HA from soils, due to its great

agronomic importance (dos Santos et al., 2020; Bento et al., 2020; Canellas and Façanha, 2004; da Silva et al., 2020; Nebbioso and Piccolo, 2011; Novotny et al., 2009; Senesi et al., 2003; Tadini et al., 2020; Vergnoux et al., 2011). FA also have a great influence on soil functionality, however, the amount of studies regarding FA from soils in the literature is less compared to HA.

FA plays an important role in the mobility of metal ions, affecting their distribution, toxicity, and bioavailability in soils (Tadini et al., 2020; Zhu and Ryan, 2016; Zhu et al., 2014). Thus, the study of its role in the environment is also of great value. This fraction of HS is the most reactive, and the most mobile, due to its solubility with an abundance of oxygen-functional groups, that are responsible for the high complexation capacity with metals, especially copper ions (Tadini et al., 2020; Esteves da Silva et al., 1998). Copper is an essential micronutrient for plant growth and development, but both excess and lack can be harmful (Yruela, 2005). Therefore, maintaining adequate concentrations of this element is necessary.

The chelating properties of FA can either reduce toxicity when there is an excess of copper, or prevent it from precipitating as insoluble hydroxide, which renders it inaccessible to the plant (Boguta and Sokołowska, 2020; Bertoli et al., 2016; Stevenson, 1994). Tadini et al. (2020) studied the interaction of copper with FA from Amazonian Spodosols. The FA showed greater interaction and quantity of complexation sites over the soil profile than the HA obtained from the same local. Moreover, the effect of the addition of pig slurry on the complexation properties of FA from a Calcic Luvisol was evaluated by the FA interaction with copper (Plaza et al., 2005). It was observed that the amendment with pig slurry decreased the binding affinity and complexation capacity of soil FA compared to the control, and this observation was explained by the decrease in oxygenated functional groups in FA. In addition, different soils have different

proportion of functional groups, which leads to changes in affinity for metals. Therefore, since soil functionality depends on this, it is important to understand the molecular composition of FA, and how it interacts with metallic ions.

Fluorescence excitation-emission matrix (EEM) coupled to parallel factor analysis (PARAFAC) has proved to be a powerful technique to investigate the binding properties between organic matter with metallic species, and this due to the high sensitivity, low cost and low sample volume (dos Santos et al., 2020; Tadini et al., 2020; Yuan et al., 2015; Mounier et al., 2011; Stedmon and Bro, 2008). Further, because different chemical species have different fluorescence lifetimes, it is also possible to study the fluorescence quenching mechanism through time-resolved fluorescence (TRF). Thereby, the possible mechanisms includes dynamic or static quenching (dos Santos et al., 2020; Nouhi et al., 2018).

Thus, the aim of this study was the molecular characterization of fulvic acids extracted from *Terra Mulata* soils. In addition, the interaction of fulvic acids with Cu(II) ions were assessed by fluorescence quenching and time-resolved fluorescence in order to provide quantitative data on the complexation capacity, conditional stability constant and complexation mechanism. And, in the end, provide subsidies for those seeking to understand the intrinsic characteristics of these soils to later try to mimic experimentally the chemical nature of its organic matter.

2. Materials and Methods

2.1 *Terra Mulata* sampling

Soil sampling was performed following the 2000 United States Environmental Protection Agency method (US EPA, 2000). Two different sampling areas of TM were selected: the first one is from an open area, covered with native and low vegetation (called TM I; 3°04′05.45″ S and 58°33′51.11″ W) and the second one is from a closed

area with native vegetation (called TM II; 3°04′05.17″ S and 58°34′11.68″ W). All areas are located near Itacoatiara city, in Amazonas State (Brazil) (SISBio collection authorization by the Chico Mendes Institute for Biodiversity Conservation, n° 50042 -2 and registration in the National System for the Management of Genetic Heritage and Associated Traditional Knowledge (SisGen), No. A0018C2). Soil samples were collected from layers, 0 to 30 cm deep, air-dried, and sieved through a 2 mm mesh to remove roots and fragments. Soil characterization can be found in Oliveira et al. (2018) and Santana et al. (2019).

2.2 Extraction of fulvic acids

The FA extractions were performed following the International Humic Substances Society (IHSS) recommendations (Swift, 1996). HS were extracted from TMs in a proportion of 1:10 (soil:extractor), using 0.1 mol L^{-1} NaOH aqueous solution under N_2 in a mechanical shaking for 4 h. The alkaline extracts were separated by centrifugation. Therefore, the solutions were acidified with 6 mol L^{-1} HCl aqueous solutions until pH~1 was achieved. This procedure was carried out to separate the HA and FA fractions: HA fraction was precipitated while FA remained in the supernatant. Subsequently, this solid-liquid mixture was centrifuged. For FA purification an adsorption resin (XAD-8) was used, and the alkaline elution passed through a cation exchange resin (Amberlite IR 120, H^+ form). Subsequently, the extracts of FA were freeze-dried for further analysis.

2.3 Characterization of fulvic acids

2.3.1 Elemental analysis

Elemental analyses of FA were performed on solids using an Elemental Analyzer instrument (2400 Series II CHNS/O, Perkin Elmer, Walther, Massachusetts,

USA). Two replicates were performed for each sample. The ash content was determined in a muffle furnace at 750 ºC for 4 h (three replicates). The O content was obtained as shown in Equation 1. After, C, H, N, S, and O contents were recalculated on an ash-free basis. The H/C and O/C atomic ratios were determined from elemental analysis (dos Santos et al., 2020; Giovanela et al., 2010; Stevenson, 1994).

$$O\% = 100\,\% - (C\%, H\%, N\%, S\% + ashes\%) \quad (1)$$

2.3.2 Infrared spectroscopy

Infrared spectra were obtained using a spectrophotometer coupled with an attenuated total reflectance (ATR) accessory equipped with a single reflection diamond crystal (ATR-FTIR) (Perkin Elmer, Spectrum Two UATR, USA). The solid material was placed directly on the ATR crystal and analyzed using the 4000-400 cm^{-1} spectral range with 20 scans and a resolution of 4 cm^{-1}.

2.3.3 Solid-state ^{13}C–CPMAS–NMR spectroscopy

The ^{13}C–CPMAS-NMR of FA was performed employing a Bruker AVANCE 400 MHz spectrometer (Bruker, Billerica, MA, USA) equipped with a magic angle spin (MAS) probe. A zircon cylindrical rotor with a diameter of 4.0 mm was packed with 80 mg of sample. The spectra were acquired using a rotor rotation frequency of 10 kHz, 1 s of recycle time, a contact time of 1 ms and 5000 scans. The spectral areas were integrated and divided into six chemical shifts: alkyl C (0-44 ppm), OCH_3/NCH (44-64 ppm), O-alkyl C (64-93 ppm), anomeric C (93-113 ppm), aromatic C (113-160 ppm) and carbonyl C (160-200 ppm) (Hu et al., 2019; Xu et al., 2017).

2.4 Interaction of fulvic acids with Cu(II)

2.4.1 Fluorescence quenching

The interaction of Cu(II) with FA was studied by fluorescence quenching. The concentration of FA in all experiments was kept constant at 10 mg L^{-1}. Twelve solutions with different concentrations of Cu(II) ($Cu(ClO_4)_2 \cdot 6H_2O$; Sigma-Aldrich, 98%), ranging from 0 to 11.2 mg L^{-1} were added to FA solution in a buffer medium with 0.1 mol L^{-1} HEPES (4-(2-hydroxyethyl)-1-piperazineethanesulfonic acid) at pH 7.0. The equilibrium time was determined based on the changes in the fluorescence signal and was kept at 30 min. EEM spectra were obtained on a spectrofluorometer (F4500, Hitachi, USA) equipped with a xenon lamp (450 W). The spectra were acquired in the scanning ranges 220-700 nm for emission and 220-500 nm for excitation. The excitation and emission slits were fixed at 5 nm, the scan speed was set at 2400 nm min^{-1}, and the detector voltage was 700 V. The EEM spectra obtained were treated using the chemometric tool known as parallel factor analysis (PARAFAC). The number of components responsible for fluorescence was assessed by the core consistency diagnostic (CORCONDIA) (dos Santos et al., 2020; Mounier et al., 2011). In addition, the complexation parameters were determined by the optimization proposed by Ryan and Weber (1982), as simplified by Equation 2.

$$I = \left(\frac{(I_{res} - 100)}{2KC_L}\right)\left[(KC_L + KC_M + 1) - \sqrt{(KC_L + KC_M + 1)^2 - 4K^2C_LC_M}\right] + 100 \qquad (2)$$

where I is the fluorescence intensity during the titration process, I_{res} is the residual fluorescence intensity, K is the conditional stability constant, C_M and C_L represents the total concentration of metal and ligand in mol L^{-1} in the solution system, respectively.

Both C_L, K and I_{res} where optimized to give the smallest residue between theoretical and experimental values.

2.4.2 Time-resolved fluorescence

Through the results of fluorescence quenching, three samples out of twelve were selected for lifetime measurements, i.e., three samples containing different copper concentrations for each FA interaction. The first one contained no copper (C_0) and two others contained 0.7 mg L^{-1} ($C_{0.7}$) and 5.6 mg L^{-1} ($C_{5.6}$), respectively. Before each measurement, the sample was bubbled with nitrogen for at least 10 min to avoid photodegradation by dissolved O_2 (dos Santos et al., 2020). The excitation wavelength was at 266 nm corresponding to the fourth harmonic of a nanosecond laser Nd:YAG (Quanta-Ray INDI, Spectra Physic, Germany), for which excitation (1024 nm) occurred with a pulse width of 5 ns and a repetition of 20 Hz. The fluorescence signal was detected using an intensified charge-coupled device (CCD) camera with a 35 ns gate width and six hundred spectra were accumulated at each time step of 0.2 ns. The spectral deconvolution and associated lifetime values were obtained by using a homemade MATLAB® program.

3. Results and discussion

3.1 Characterization of fulvic acids

Table 1 lists the elemental composition, atomic ratios and ashes of fulvic acids from the two soil areas. In general, both FA samples, from TM I and TM II, showed oxygen as the main constituent (62.68 and 57.94, respectively), followed by carbon, hydrogen, nitrogen, and sulfur. This trend is not common for FA (oxygen content higher than carbon), but can also be seen in Xiaoli et al. (2008). As there are no other studies in

the literature on FA from *Terra Mulata* soils, this fact is attributed to the intrinsic characteristics of the samples. To further investigate the characteristics of the FA samples, the H/C and O/C atomic ratios were calculated from the elemental analysis. These ratios are related to the degree of aromatic rings condensation and the content of oxygen-functional groups, respectively (Giovanela et al., 2010; Stevenson, 1994). Higher values for H/C atomic ratios were found in the FA from TM compared to the FA extracted from Cambisols, Podzols and Chernozems, located in China, Italy and Canada, respectively (Limura et al., 2012), indicating more contribution of alkyl chains in FA from TM. The same behavior (higher values) were found for the O/C atomic ratio in the FA from TM, indicating more contribution of oxygen-functional groups (Limura et al., 2012).

Table 1. Weight percentage (*) of carbon (C), hydrogen (H), nitrogen (N), oxygen (O), sulfur (S) and ash contents, as well as O/C and H/C atomic ratios for FA from TM.

FA	C (%)	H (%)	N (%)	O (%)	S (%)	O/C	H/C	Ash (%)
TM I	31.32	3.21	1.38	62.68	1.40	1.50	1.23	6.89±0.19
TM II	35.68	3.54	1.71	57.94	1.13	1.22	1.19	6.23±0.24

*Ash-free basis

The FTIR spectra of FA are shown in Fig. 1. In general, both spectra are slightly similar. The broad and intense band in the range of 3500-3000 cm^{-1} is related to O-H stretching vibration of alcohols, carboxylic acids, phenols and also N-H stretching vibration of amide or amine groups (Vergnoux et al., 2011). It can be seen in the region of 3000-2800 cm^{-1} bands corresponding to alkyl stretching vibration, which was more evident for FA from TM 1 (Li and Wu, 2013; Vergnoux et al., 2011). In addition, the

250 absorption near 2500 cm^{-1} could be attributed to carboxylic acids dimers formed by
251 hydrogen-bonds (Bertoli et al., 2016).

252 In the region of 2000 to 1000 cm^{-1} it is difficult to precisely interpret due to the
253 various overlapping bands. Therefore, for a better interpretation of the infrared spectra,
254 Fig. S1 shows the second derivative curves. This tool has been used to separate
255 broadband absorption peaks of complex matrices which show new peaks that were
256 previously imperceptible (Tinti et al., 2015). In the 1700 cm^{-1} region it is possible to
257 observe bands in 1791 cm^{-1} and 1711 cm^{-1} related to the C=O stretching of carboxylic
258 acids. This is the most intense and well defined band observed for both FA. In addition,
259 the aromatic portion of AF can be observed by the appearance of the bands near 1620
260 and 1530 cm^{-1} in the second derivative curves (Fig. S1), which was not previously
261 shown in the original spectra (Fig. 1) (Gondar et al., 2005). Additionally, the band near
262 1420 cm^{-1} was associated to vibrations of C-H in methylene groups.

263 The contribution of carbohydrate-like compounds to the composition of FA can
264 be assessed by the appearance of bands referring to the asymmetric stretch of C-O-C
265 and C-O (around 1200 and 1100 cm^{-1}). Further, the bands at 1055 cm^{-1} and 1080
266 cm^{-1} may have diverse origin. It may be either from C-O stretching or O-H groups, and
267 even vibration of minerals, such as Si-O (Drosos et al., 2009; Giovanela et al., 2010;
268 Stevenson, 1994).

269

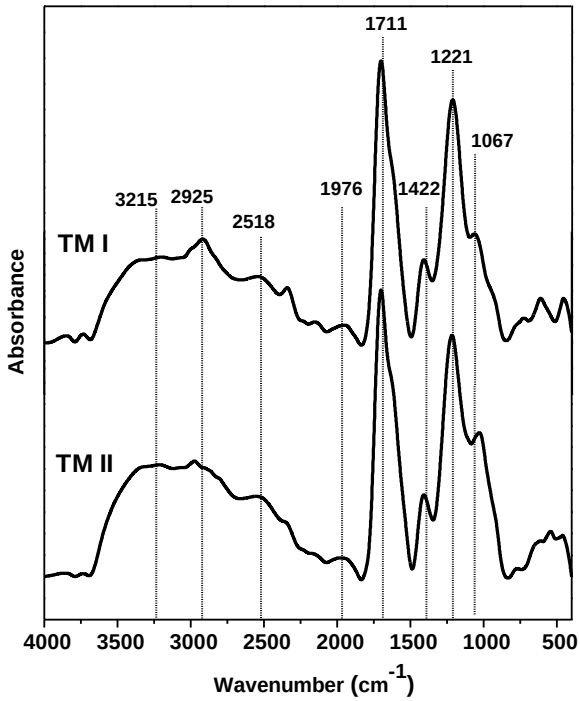

Fig. 1. FTIR spectra for FA extracted from TM soils.

As shown in Fig. 2, the ^{13}C-CPMAS-NMR spectra of both FA exhibited the same peaks. The results revealed the presence of alkyl and aromatic carbons, substituted or not by heteroatoms and all chemical shifts were consistent with those observed in soil FA by other authors (Hu et al., 2019; Xu et al., 2017; Xiaoli et al., 2008). Besides, the spectra could be divided into six regions assigned to signals from alkyl C (0-44 ppm), OCH_3/NCH (44-64 ppm), O-alkyl C (64-93 ppm), anomeric C (93-113 ppm), aromatic C (113-160 ppm) and carbonyl C (160-200 ppm) (Hu et al., 2019; Xu et al., 2017).

Chemical shifts near 37 ppm were assigned to long chain $(CH_2)_n$ similar to those present in cutin, suberin, and plant waxes (Lorenz et al., 2000). This peak was evident in both FA. Furthermore, the peaks, in the 71-74 ppm range, centered at 72 ppm, were attributed to the overlapping of carbons number 2, 3 and 5 in the pyranosidic cellulose and hemicellulose structures. In addition, the signal at 130 ppm was assigned to unsubstituted aromatic carbons in FA structures. The major peak at 172 ppm

represented the carbonyl C of carboxylic acid, ester and amide (Hu et al., 2019; Xiaoli et al., 2008), suggesting a high content of these functional groups.

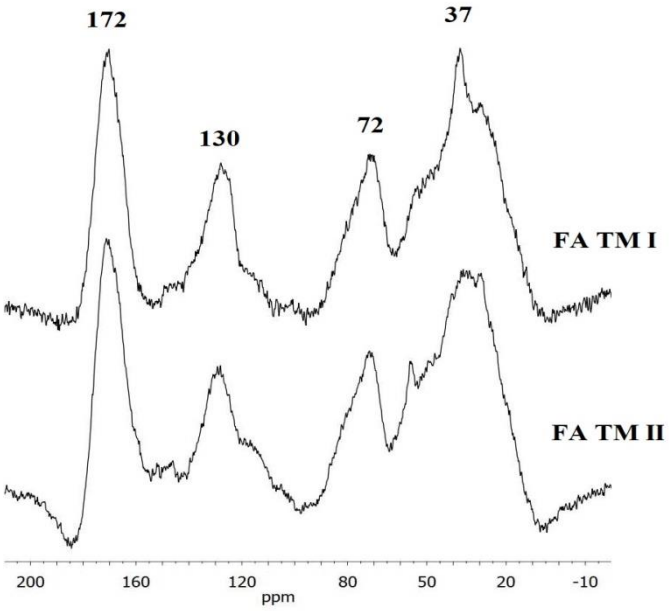

Fig. 2. Solid-state ^{13}C-CPMAS-NMR spectra of FA samples.

The total area integration of spectra, made to obtain the relative intensity of each chemical shift, is shown in Table 2. The results revealed that alkyl and carbonyl functional groups were the dominant carbon components in FA structures, followed by aromatic C, OCH_3/NCH, O-alkyl C, and anomeric C. As for the infrared analysis, both FA also had a very similar composition according to the ^{13}C NMR results. A small difference can be observed between samples, in which the FA from TM I have a slight increase in oxygenated groups and a slight decrease in hydrophobic functional groups, such as the aromatic and alkyl portions, and this when compared to the FA from TM II. This trend could also be seen through the H/C and O/C atomic ratios.

Table 2. Relative value (% of total area) obtained from ^{13}C-CPMAS-NMR spectra of FA samples.

	^{13}C NMR region (ppm)					
FA	**200-160**	**160-113**	**113-93**	**93-64**	**64-44**	**44-0**
TM I	19.29	16.40	0.32	15.76	16.08	32.15
TM II	17.82	17.82	0.33	14.85	16.17	33.00

Therefore, as previously reported, stable alkyl structures, rich in oxygen-functional groups were found in the FA structures (Jouraiphy et al., 2008). In this study, it was possible to observe the same patterns in ^{13}C NMR, infrared and elemental analysis. In addition, greater functionalization was observed in FA from TM compared to other FA in the literature (Gondar et al., 2005; Lorenz et al., 2000; Xiaoli et al., 2008; Xu et al., 2017). The presence of these functional groups (carbonyl, carboxyl, hydroxyl, phenolic and aromatic portions) is extremely important, since they could act as reactive sites in metal complexation reactions, and, in addition, reaffirms the particularity of this kind of soil and the importance of FA in soil systems.

3.2 Interaction of fulvic acids with Cu(II)

3.2.1 Fluorescence quenching

The interaction of FA from TM I and TM II with Cu(II) ions was studied by fluorescence quenching, in which a two-component model was found for Cu(II)-FA with a good CORCONDIA value (98.80%) (Fig. 3a and b). The first component (Fig. 3a) had a main peak at [λ_{Ex} 260nm/λ_{Em} 430nm] and the second one at [λ_{Ex} 310nm/λ_{Em} 430nm], which is characteristic of fulvic acids from soil (Tadini et al., 2019). These peaks were at shorter emission wavelengths and in the blue region of the visible

spectrum, characterizing the presence of simple structures in FA samples (Senesi et al., 2003), such as alkyl groups. This corroborates with the ^{13}C NMR measurement, H/C atomic ratio, and FTIR spectra, showing a high content of this functional group.

Fulvic acids has blue shifts for emission wavelengths compared to humic acids from the same origin (Sierra et al., 2000). Generally, the blue-shift phenomenon is attributed to the presence of more alkyl structures in samples. Emission fluorescence intensity in longer wavelengths were shown in humic acids from TM, the same soils used in this study (dos Santos et al., 2020). The fluorescence intensity in longer wavelengths is due to the presence of more aromatic structures, which, in the literature, is called red-shift.

The second component (Fig. 3b) presented a continuous emission range, showing no variation of its contribution during quenching experiments. This component is probably related to a noise factor in the UV domain (<250nm). Thus, this component was not included in the discussion.

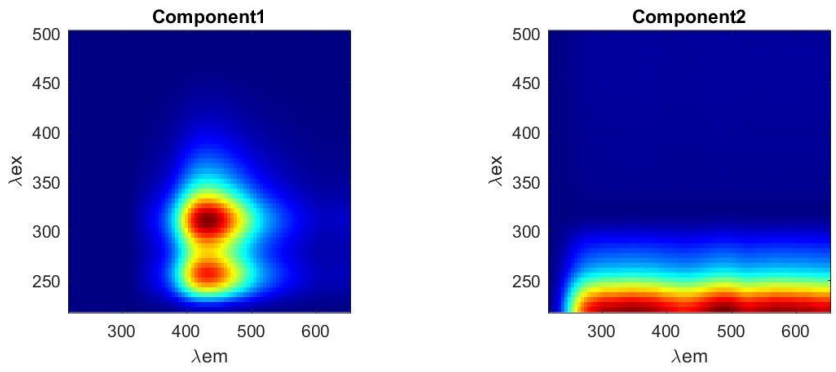

(a) (b)

Fig. 3. Components 1 (a) and 2 (b) obtained by PARAFAC for interaction of FA with Cu(II).

The data optimization using the 1:1 (ligand:metal) complexation model proposed by Ryan and Weber (1982) allowed the quantitative evaluation of fluorescence quenching. Bias was used as an optimization parameter. Mounier et al. (2011) defined Bias as the sum of the absolute value of the difference between the experimental, and the calculated fluorescence intensity. In this study, Bias values ranged from 2.02 to 2.29 (Table 3), which are lower than others found in the literature (Tadini et al., 2020), indicating that experimental results fit well to theoretical model. Moreover, the titration curves of component 1 referring to FA from TM I is presented in Fig. 4. The symbols represent the data obtained experimentally and the solid line show the theoretical values as a function of Cu(II) addition. FA from TM II showed the same behavior (Fig. S2).

The fluorescence quenching curve for FA from TM I and Cu(II) showed a fluorescence intensity decay of approximately 84% (Fig. 4). The quenching effect was strongest at the initial doses of copper (higher slope of the curve), where there were a large number of active sites that are now coordinating copper, thus forming complexes (Boguta et al., 2019; Mounier et al., 2011). In addition, the decrease of fluorescence contribution with increased metal concentration suggested the saturation of accessible sites, and the fact that the decay did not fall to zero is due to some fluorophores that did not participate in Cu(II) binding (Boguta et al., 2019; Boguta and Sokołowska, 2020).

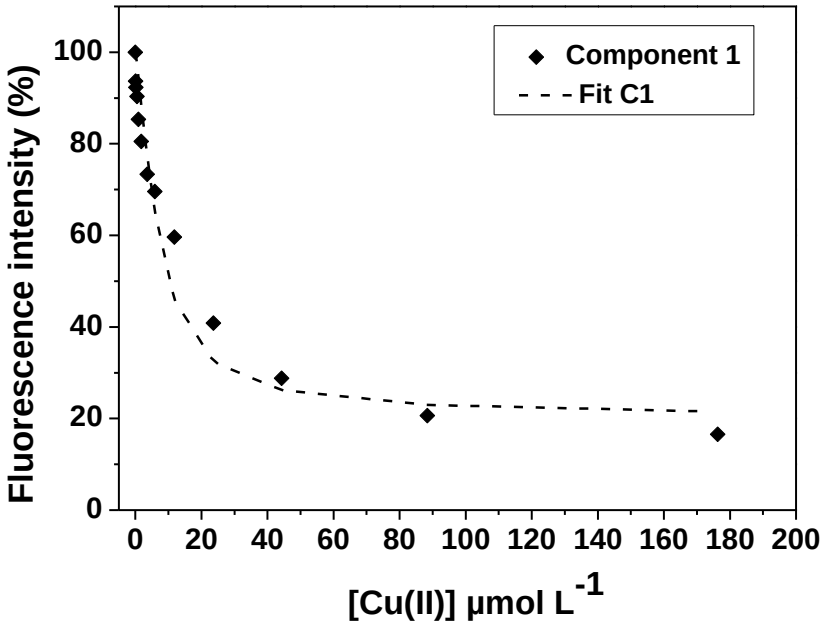

Fig. 4. Fluorescence quenching curve of FA from TM I determined experimentally (symbol) compared with the theoretical (dash line) as a function of Cu(II) addition.

The proposed complexation model allowed the calculation of C_L and K, where C_L represents the concentration of binding sites available for interaction with Cu(II) ions and K is the conditional stability constant of the complex formed. The Log K values were 5.57 and 5.38 for the FA components from TM I and II, respectively (Table 3). These values were higher than those found for FA extracted from Amazonian Spodosol (Tadini et al., 2020), Oak Forest soil (Esteves da Silva et al., 1998) and the standard FA of Elliot Soil (IHSS sample) (Enev et al., 2016), indicating that the complex formed between TM FA and Cu(II) is more stable (Table 3). In addition, high stability constant values were reported for the interaction of humic acids also extracted from TM with Cu(II), then demonstrating that both humic fractions present a great affinity to interact with this metal (dos Santos et al., 2020). The complexation capacity (C_C) was obtained by dividing the C_L values, in mol L^{-1}, by the carbon concentration calculated from the FA carbon content, in mg C L^{-1}, and represents the density of binding sites (in mol) for a metal (Cu(II)) per gram of carbon in the organic matter

(fulvic acids). Therefore, the C_C values calculated for FA components from TM I and II were 1.43 and 2.09 mmol of Cu(II) g^{-1} C, respectively (Table 3). These values were also higher than the other FA found in the literature (Esteves da Silva et al., 1998; Tadini et al., 2020), suggesting a high concentration of binding sites available to interact with Cu(II) ions (Table 3).

Gathering the results, both FA from TM showed a high quantity of binding sites, as well as an affinity for interaction with Cu(II), then, acting in complexation reactions and consequently the bioavailability of copper. Generally, paramagnetic metal ions, such as Cu(II), display high stability constants values with FA. It may be explained by the $3d^9$ configuration of the divalent copper with incomplete d orbitals. In addition, studies indicate that the high stability constant for the complex formed is associated with the increase of acidic functional groups and other oxygen-containing ligand groups (Guo et al., 2012, 2015). Oxygen is a Lewis base, a small atom and electron donor in carboxyl, carbonyl and hydroxyl groups. Exhibit high electronegativity, and form strong bonds with small Lewis acids, such as Cu(II) (Pearson's rule). These oxygenated functional groups were observed for FA, as shown in ^{13}C NMR, FTIR and Elemental Analysis. So, FA had good interaction with Cu(II) due to its molecular structure. Therefore, these results are important for understanding the mobility and fate of copper in the environment.

Table 3. Conditional stability constant (Log K) and complexation capacity (C_C) for component 1 regarding the interaction of FA from *Terra Mulata* with Cu(II) ions and other FA extracted from soils reported in the literature.

Soil	Metal	Method	Conditional stability constant (Log K)	Complexation capacity (C_C) (mmol Cu(II) g^{-1} C)	Reference
Terra Mulata I	Cu(II)	Ryan and Weber	5.57	1.43	This study
Terra Mulata II	Cu(II)	Ryan and Weber	5.38	2.09	This study
Amazonian Spodosol	Cu(II)	Ryan and Weber	2.26–5.31	0.11–2.44	(Tadini et al., 2020)
Oak Forest	Cu(II)	Ryan and Weber	4.33–4.60	0.03–0.04	(Esteves da Silva et al., 1998)
Elliot soil (IHSS sample)	Cu(II)	Stern-Volmer	4.45	-	(Enev et al., 2016)

- not realized

3.2.2 Time-resolved fluorescence

The quenching process can be induced by two mechanisms. The first one is static quenching, with the formation of a non-fluorescent ground-state complex, where the lifetime of the complex is not affected. The second one is dynamic quenching, which is caused by collision with a quencher and fluorophore during the lifetime of the excited state, thus, affecting the fluorescence lifetime (Lakowics, 1999). Therefore, as a complementary technique to fluorescence quenching, TRF was used to assess the interaction mechanism between FA from TM and Cu(II) and distinguish whether a static or dynamic quenching process occurred. Furthermore, to the best of our knowledge, this kind of analysis for any FA from TM is not in the literature, thus, highlighting the importance of this analysis.

Fig. S4 shows the fluorescence lifetime distribution of FA complexes with copper. Through the deconvolution results, the decay was found to be mono-exponential (τ_1), i.e., containing only one lifetime. For both FA the average lifetime values observed were approximately 5.0 ± 0.2 ns. These results fit well with the PARAFAC, in which the lower lifetime can be associated with component 1 (Fig. 3a), which has a simpler fluorophore structure.

Therefore, the average lifetime values appeared to be independent of metal addition (Fig. S4). This suggests that the mechanism of fluorescence quenching between Cu(II) and FA occurred by static quenching, with a non-fluorescent ground-state complex. Nouhi (2018) reported different lifetime values, but also static quenching between Cu(II) with FA extracted from the Saint Lawrence Estuary in Canada. This is because different samples have different fluorescence decay, showing the high sensitivity and selectivity of TRF. Further, dos Santos (2020) determined the fluorescence lifetime for the interaction of humic acids from TM and Cu(II). Static

quenching was also the predominant complexation mechanism and, when compared to this study, similar values were found for τ_1.

In addition, the study of soils in terms of their complexation properties is of great value and provides important information regarding the fate of metals in the environment. TM is considered as a model of fertile soil, and researchers have been focusing on trying to reproduce this kind of soil in the laboratory, or at least, reproducing its characteristics (Cernansky, 2015). Techniques such as hydrothermal carbonization has been explored as an alternative to reproduce this anthropogenic soil particularities (dos Santos et al., 2020; Fregolente et al., 2020; Bisinoti et al., 2019; Bento et al., 2019; Santana et al., 2019; Melo et al., 2017; Silva et al., 2017; Kambo and Dutta, 2015). Therefore, it is essential to know the intrinsic characteristics of TM and this study can be a guide for those who seek to mimic these properties. Furthermore, there are no previous studies regarding the molecular characterization of fulvic acids from *Terra Mulata* soils, as well as its interaction with metallic species. This shows the novelty of the present work, as it brings brand new information about TM, from one of the sites in the Amazon basin. In addition, by showing their great capacity to interact with metallic species, the capacity of the technique to measure this and, by providing new information about the mechanism of complexation, the importance of focusing on the study of FA is demonstrated, as no information is available in the current literature about this.

4. Conclusion

The fulvic acids extracted from *Terra Mulata* soils were mainly composed of alkyl and oxygen-functional groups. The excitation-emission fluorescence spectroscopy coupled to PARAFAC showed that simple structures and less aromatic, which emit

fluorescence at low emission wavelengths, were responsible for the fluorescence phenomena, corroborating with the information presented in the structural analysis. High complexation capacity and strong binding ability were obtained between Cu(II) and fulvic acids from *Terra Mulata* soils when compared to other fulvic acids in the literature. This was due to the fact that the organic matter is well functionalized, with abundance in carboxyl, carbonyl and hydroxyl groups. Thus, the results showed that the complexation reactions are strongly correlated to the nature of the organic matter present in the soil. Furthermore, the interaction mechanism of fluorescence quenching that occurred between fulvic acids and Cu(II) was static quenching, with a non-fluorescent ground state complex formation.

This study sought to advance the knowledge of the chemical composition and binding properties of fulvic acids from *Terra Mulata* soils with metals. Therefore, these findings represent a breakthrough for those who seek to reproduce the intrinsic characteristics of Amazonian anthropogenic soils.

Acknowledgments

This work was supported by the São Paulo Research Foundation (FAPESP) (grants 15/22954-1, 17/26718-6, and 18/15733-7). J.V.S acknowledges a scholarship from FAPESP (grants 17/05408-9 and 18/09914-9). O.P.F. acknowledges financial support from Fundação Cearense de Apoio ao Desenvolvimento Científico e Tecnológico (FUNCAP) for financial support through the Grant PRONEX PR2-0101-00006.01.00/15 and also to Conselho Nacional de Desenvolvimento Científico e Tecnológico (CNPq) through the Grant 313637/2019-9 (CNPq DT 29/2019). M.C.B. acknowledges financial support from Conselho Nacional de Desenvolvimento Científico e Tecnológico (CNPq) through the Grant 303377/2019-4. The authors thank

Dr. Maurício Boscolo for offering assistance with the FTIR analysis (FAPESP, grant 2017/13230-5) and Dr. Isabella Constatino and Dr. Fabiana Paschoal for their assistance with soil sampling. Also thank to Dr. Redon Roland (roland.redon@univ-tln.fr) for the progmeef program allowing easy and rapid deconvolution time-resolved spectra.

References

Archanjo, B.S., Araujo, J.R., Silva, A.M., Capaz, R.B., Falcão, N.P.S., Jorio, A., Achete, C.A., 2014. Chemical analysis and molecular models for calcium-oxygen-carbon interactions in black carbon found in fertile amazonian anthrosoils. Environ. Sci. Technol. 48, 7445–7452. https://doi.org/10.1021/es501046b

Baird, C., Cann, M., 2012. Environmental Chemistry, 5th Editio. ed. New York.

Batjes, N.H., Dijkshoorn, J.A., 1999. Carbon and nitrogen stocks in the soils of the Amazon Region. Geoderma 89, 273–286. https://doi.org/10.1016/S0016-7061(98)00086-X

Bento, L.R., Castro, A.J.R., Moreira, A.B., Ferreira, O.P., Bisinoti, M.C., Melo, C.A., 2019. Release of nutrients and organic carbon in different soil types from hydrochar obtained using sugarcane bagasse and vinasse. Geoderma 334, 24–32. https://doi.org/10.1016/J.GEODERMA.2018.07.034

Bento, L.R., Melo, C.A., Ferreira, O.P., Moreira, A.B., Mounier, S., Piccolo, A., Spaccini, R., Bisinoti, M.C., 2020. Humic extracts of hydrochar and Amazonian Dark Earth: Molecular characteristics and effects on maize seed germination. Sci. Total Environ. 708, 135000. https://doi.org/10.1016/j.scitotenv.2019.135000

Bertoli, A.C., Garcia, J.S., Trevisan, M.G., Ramalho, T.C., Freitas, M.P., 2016. Interactions fulvate-metal (Zn2+, Cu2+ and Fe2+): theoretical investigation of

thermodynamic, structural and spectroscopic properties. BioMetals 29, 275–285. https://doi.org/10.1007/s10534-016-9914-8

Bisinoti, M.C., Moreira, A.B., Melo, C.A., Fregolente, L.G., Bento, L.R., dos Santos, J.V., Ferreira, Odair Pastor, 2019. Application of Carbon-Based Nanomaterials as Fertilizers in Soils, in: Nascimento, R.F., Ferreira, O. P., Paula, A.J., Neto, V.O.S. (Eds.), Nanomaterials Applications for Environmental Matrices: Water, Soil and Air. Amsterdam, pp. 305–333. https://doi.org/10.1016/B978-0-12-814829-7.00008-2

Boguta, P., D'Orazio, V., Senesi, N., Sokołowska, Z., Szewczuk-Karpisz, K., 2019. Insight into the interaction mechanism of iron ions with soil humic acids. The effect of the pH and chemical properties of humic acids. J. Environ. Manage. 245, 367–374. https://doi.org/10.1016/j.jenvman.2019.05.098

Boguta, P., Sokołowska, Z., 2020. Zinc binding to fulvic acids: Assessing the impact of pH, metal concentrations and chemical properties of fulvic acids on the mechanism and stability of formed soluble complexes. Molecules 25. https://doi.org/10.3390/molecules25061297

Canellas, L.P., Façanha, A.R., 2004. Chemical nature of soil humified fractions and their bioactivity. Pesqui. Agropecu. Bras. 39, 233–240. https://doi.org/10.1590/S0100-204X2004000300005

Cernansky, R., 2015. State of the art soil. Nature 517, 258–260. https://doi.org/10.1038/517258a

Clement, C.R., Denevan, W.M., Heckenberger, M.J., Junqueira, A.B., Neves, E.G., Teixeira, W.G., Woods, W.I., 2015. The domestication of amazonia before european conquest. Proc. R. Soc. B Biol. Sci. 282.

https://doi.org/10.1098/rspb.2015.0813

Coe, M.T., Marthews, T.R., Costa, M.H., Galbraith, D.R., Greenglass, N.L., Imbuzeiro, H.M.A., Levine, N.M., Malhi, Y., Moorcroft, P.R., Muza, M.N., Powell, T.L., Saleska, S.R., Solorzano, L.A., Wang, J., 2013. Deforestation and climate feedbacks threaten the ecological integrity of south-southeastern Amazonia. Philos. Trans. R. Soc. B Biol. Sci. 368. https://doi.org/10.1098/rstb.2012.0155

Cunha, T.J.F., Madari, B.E., Canellas, L.P., Ribeiro, L.P., Benites, V. de M., Santos, G. de A., 2009. Soil organic matter and fertility of anthropogenic dark earths (Terra Preta de Índio) in the Brazilian Amazon basin. Rev. Bras. Ciência do Solo 33, 85–93. https://doi.org/10.1590/s0100-06832009000100009

da Silva, L.S., Constantino, I.C., Bento, L.R., Tadini, A.M., Bisinoti, M.C., Boscolo, M., Ferreira, O.P., Mounier, S., Piccolo, A., Spaccini, R., Cornélio, M.L., Moreira, A.B., 2020. Humic extracts from hydrochar and Amazonian Anthrosol: Molecular features and metal binding properties using EEM-PARAFAC and 2D FTIR correlation analyses. Chemosphere 256, 1–12. https://doi.org/10.1016/j.chemosphere.2020.127110

dos Santos, J.V., Fregolente, L.G., Moreira, A.B., Ferreira, O.P., Mounier, S., Viguier, B., Hajjoul, H., Bisinoti, M.C., 2020. Humic-like acids from hydrochars: Study of the metal complexation properties compared with humic acids from anthropogenic soils using PARAFAC and time-resolved fluorescence. Sci. Total Environ. 722, 137815. https://doi.org/10.1016/j.scitotenv.2020.137815

Drosos, M., Jerzykiewicz, M., Deligiannakis, Y., 2009. H-binding groups in lignite vs. soil humic acids: NICA-Donnan and spectroscopic parameters. J. Colloid Interface Sci. 332, 78–84. https://doi.org/10.1016/j.jcis.2008.12.023

Enev, V., Türkeová, I., Szewieczková, J., Doskočil, L., Klučáková, M., 2016. Fluorescence analysis of Cu(II), Pb(II) and Hg(II) ion binding to humic and fulvic acids. Mater. Sci. Forum 851, 135–140. https://doi.org/10.4028/www.scientific.net/MSF.851.135

Esteves da Silva, J.C.G., Machado, A.A.S.C., Ferreira, M.A., Rey, F., 1998. Method for the differentiation of leaf litter extracts and study of their interaction with Cu(II) by molecular fluorescence. Can. J. Chem. 76, 1197–1209. https://doi.org/10.1139/cjc-76-8-1197

Fraser, J., Teixeira, W., Falcão, N., Woods, W., Lehmann, J., Junqueira, A.B., 2011. Anthropogenic soils in the Central Amazon: From categories to a continuum. Area 43, 264–273. https://doi.org/10.1111/j.1475-4762.2011.00999.x

Fregolente, L.G., de Castro, A.J.R., Moreira, A.B., Ferreira, O.P., Bisinoti, M.C., 2020. New Proposal for Sugarcane Vinasse Treatment by Hydrothermal Carbonization: An Evaluation of Solid and Liquid Products. J. Braz. Chem. Soc. 31, 40–50.

Giovanela, M., Crespo, J.S., Antunes, M., Adamatti, D.S., Fernandes, A.N., Barison, A., Da Silva, C.W.P., Guégan, R., Motelica-Heino, M., Sierra, M.M.D., 2010. Chemical and spectroscopic characterization of humic acids extracted from the bottom sediments of a Brazilian subtropical microbasin. J. Mol. Struct. 981, 111–119. https://doi.org/10.1016/j.molstruc.2010.07.038

Glaser, B., Balashov, E., Haumaier, L., Guggenberger, G., Zech, W., 2000. Black carbon in density fractions of anthropogenic soils of the Brazilian Amazon region. Org. Geochem. 31. https://doi.org/10.1016/S0146-6380(00)00044-9

Gondar, D., Lopez, R., Fiol, S., Antelo, J.M., Arce, F., 2005. Characterization and acid-base properties of fulvic and humic acids isolated from two horizons of an

574 ombrotrophic peat bog. Geoderma 126, 367–374.
575 https://doi.org/10.1016/j.geoderma.2004.10.006

576 Guo, X., Jiang, J., Xi, B., He, X., Zhang, H., Deng, Y., 2012. Study on the spectral and
577 Cu (II) binding characteristics of DOM leached from soils and lake sediments in
578 the Hetao region. Environ. Sci. Pollut. Res. 19, 2079–2087.
579 https://doi.org/10.1007/s11356-011-0704-0

580 Guo, X. jing, Zhu, N. min, Chen, L., Yuan, D. hai, He, L. sheng, 2015. Characterizing
581 the fluorescent properties and copper complexation of dissolved organic matter in
582 saline-alkali soils using fluorescence excitation-emission matrix and parallel factor
583 analysis. J. Soils Sediments 15, 1473–1482. https://doi.org/10.1007/s11368-015-
584 1113-7

585 Hu, J., Wu, J., Sharaf, A., Sun, J., Qu, X., 2019. Effects of organic wastes on structural
586 characterizations of fulvic acid in semiarid soil under plastic mulched drip
587 irrigation. Chemosphere 234, 830–836.
588 https://doi.org/10.1016/j.chemosphere.2019.06.118

589 Jouraiphy, A., Amir, S., Winterton, P., El Gharous, M., Revel, J.C., Hafidi, M., 2008.
590 Structural study of the fulvic fraction during composting of activated sludge-plant
591 matter: Elemental analysis, FTIR and 13C NMR. Bioresour. Technol. 99, 1066–
592 1072. https://doi.org/10.1016/j.biortech.2007.02.031

593 Kambo, H.S., Dutta, A., 2015. A comparative review of biochar and hydrochar in terms
594 of production , physico-chemical properties and applications. Renew. Sustain.
595 Energy Rev. 45, 359–378. https://doi.org/10.1016/j.rser.2015.01.050

596 Lakowics, J.R., 1999. Principles of fluorescence spectroscopy, 2nd ed. New York:
597 Kluwer Academic/ Plenum Publisher.

598 Li, J. ming, Wu, J. gui, 2013. Compositional and structural difference of fulvic acid
599 from black soil applied with different organic materials: Assessment after three
600 years. J. Integr. Agric. 12, 1865–1871. https://doi.org/10.1016/S2095-
601 3119(13)60397-4

602 Limura, Y., Ohtani, T., Chersich, S., Tani, M., Fujitake, N., 2012. Characterization of
603 dax-8 adsorbed soil fulvic acid fractions by various types of analyses. Soil Sci.
604 Plant Nutr. 58, 404–415. https://doi.org/10.1080/00380768.2012.708318

605 Lorenz, K., Preston, C.M., Raspe, S., Morrison, I.K., Heinz, K., 2000. Litter
606 decomposition and humus characteristics in Canadian and German spruce
607 ecosystems: information from tannin analysis and 13C CPMAS NMR. Soil Biol.
608 Biochem. 32, 779–792. https://doi.org/10.1016/S0038-0717(99)00201-1

609 Lucheta, A.R., Cannavan, F.S., Tsai, S.M., Kuramae, E.E., 2017. Amazonian Dark
610 Earth and Its Black Carbon Particles Harbor Different Fungal Abundance and
611 Diversity. Pedosphere 27, 832–845. https://doi.org/10.1016/S1002-0160(17)60415-
612 6

613 Melo, C.A., Junior, F.H.S., Bisinoti, M.C., Moreira, A.B., Ferreira, O.P., 2017.
614 Transforming sugarcane bagasse and vinasse wastes into hydrochar in the presence
615 of phosphoric acid: an evaluation of nutrient contents and structural properties.
616 Waste and Biomass Valorization 1139–1151. https://doi.org/10.1007/s12649-016-
617 9664-4

618 Mounier, S., Zhao, H., Garnier, C., Redon, R., 2011. Copper complexing properties of
619 dissolved organic matter: PARAFAC treatment of fluorescence quenching.
620 Biogeochemistry 106, 107–116. https://doi.org/10.1007/s10533-010-9486-6

621 Nebbioso, A., Piccolo, A., 2011. Basis of a humeomics science: Chemical fractionation

622 and molecular characterization of humic biosuprastructures. Biomacromolecules
623 12, 1187–1199. https://doi.org/10.1021/bm101488e

624 Nouhi, A., 2018. Caractérisation Spectrale et Temporelle par Quenching de
625 Fluorescence des Interactions Matière Organique-Eléments Métalliques. Universté
626 de Toulon.

627 Nouhi, A., Hajjoul, H., Redon, R., Gagné, J.P., Mounier, S., 2018. Time-resolved laser
628 fluorescence spectroscopy of organic ligands by europium: Fluorescence
629 quenching and lifetime properties. Spectrochim. Acta - Part A Mol. Biomol.
630 Spectrosc. 193, 219–225. https://doi.org/10.1016/j.saa.2017.12.028

631 Novotny, E.H., Hayes, M.H.B., Madari, B.E., Bonagamba, T.J., deAzevedo, E.R., de
632 Souza, A.A., Song, G., Nogueira, C.M., Mangrich, A.S., 2009. Lessons from the
633 Terra Preta de Índios of the Amazon Region for the utilisation of charcoal for soil
634 amendment. J. Braz. Chem. Soc. 20, 1003–1010. https://doi.org/10.1590/S0103-
635 50532009000600002

636 Oliveira, N.C., Paschoal, A.R., Paula, R.J., Constantino, I.C., Bisinoti, M.C., Moreira,
637 A.B., Fregolente, L.G., Santana, A.M., Sousa, F.A., Ferreira, O.P., Paula, A.J.,
638 2018. Morphological analysis of soil particles at multiple length-scale reveals
639 nutrient stocks of Amazonian Anthrosols. Geoderma 311, 58–66.
640 https://doi.org/10.1016/j.geoderma.2017.09.034

641 Plaza, C., Senesi, N., García-Gil, J.C., Polo, A., 2005. Copper(II) complexation by
642 humic and fulvic acids from pig slurry and amended and non-amended soils.
643 Chemosphere 61, 711–716. https://doi.org/10.1016/j.chemosphere.2005.03.046

644 Ryan, D.K., Weber, J.H., 1982. Fluorescence Quenching Titration for Determination of
645 Complexing Capacities and Stability Constants of Fulvic Acid. Anal. Chem. 54,

986–990. https://doi.org/10.1021/ac00243a033

Santana, A.M., Bisinoti, M.C., Melo, C.A., Ferreira, O.P., 2019. Disponibilidade de nutrientes e carbono orgânico em solos contendo carvão hidrotérmico lavado e não lavado e comparação com solos antropogênicos. Quim. Nova 42, 262–272. https://doi.org/10.21577/0100-4042.20170339

Senesi, N., D'Orazio, V., Ricca, G., 2003. Humic acids in the first generation of EUROSOILS. Geoderma 116, 325–344. https://doi.org/10.1016/S0016-7061(03)00107-1

Sierra, M.M.S., Giovanela, M., Soriano-Sierra, E.J., 2000. Fluorescence properties of well-characterized sedimentary estuarine humic compounds and surrounding pore waters. Environ. Technol. (United Kingdom) 21, 979–988. https://doi.org/10.1080/09593332108618046

Silva, C.C., Melo, C.A., Soares Junior, F.H., Moreira, A.B., Ferreira, O.P., Bisinoti, M.C., 2017. Effect of the reaction medium on the immobilization of nutrients in hydrochars obtained using sugarcane industry residues. Bioresour. Technol. 237, 213–221. https://doi.org/10.1016/j.biortech.2017.04.004

Soares, M.R., Alleoni, L.R.F., Vidal-Torrado, P., Cooper, M., 2005. Mineralogy and ion exchange properties of the particle size fractions of some Brazilian soils in tropical humid areas. Geoderma 125, 355–367. https://doi.org/10.1016/j.geoderma.2004.09.008

Stedmon, C.A., Bro, R., 2008. Characterizing dissolved organic matter fluorescence with parallel factor analysis: a tutorial. Limnol. Oceanogr. 6, 1–8. https://doi.org/10.4319/lom.2008.6.572

669 Stevenson, F.J., 1994. Humus chemistry: Genesis, composition, and reactions. New
670 York John Wiley Sons.

671 Swift, R.S., 1996. Methods of soil analysis. Part 3. Chemical methods. Soil Sci. Soc.
672 Am. 1011–1020.

673 Tadini, A. M.; Mounier, S.; Milori, D.M.B.P., 2020. Modeling the quenching of
674 fluorescence from organic matter in Amazonian soils. Sci. Total Environ. 698,
675 134067. https://doi.org/10.1016/j.scitotenv.2019.134067

676 Tinti, A., Tugnoli, V., Bonora, S., Francioso, O., 2015. Recent applications of
677 vibrational mid-infrared (IR) spectroscopy for studying soil components: A review.
678 J. Cent. Eur. Agric. 16, 1–22. https://doi.org/10.5513/JCEA01/16.1.1535

679 US EPA, 2000. Environmental Protection Agency, Environmental Response Team.
680 Standard operating procedures – SOP 1–4.

681 Vergnoux, A., Guiliano, M., Di Rocco, R., Domeizel, M., Théraulaz, F., Doumenq, P.,
682 2011. Quantitative and mid-infrared changes of humic substances from burned
683 soils. Environ. Res. 111, 205–214. https://doi.org/10.1016/j.envres.2010.03.005

684 Xiaoli, C., Shimaoka, T., Qiang, G., Youcai, Z., 2008. Characterization of humic and
685 fulvic acids extracted from landfill by elemental composition, 13C CP/MAS NMR
686 and TMAH-Py-GC/MS. Waste Manag. 28, 896–903.
687 https://doi.org/10.1016/j.wasman.2007.02.004

688 Xu, J., Zhao, B., Chu, W., Mao, J., Zhang, J., 2017. Chemical nature of humic
689 substances in two typical Chinese soils (upland vs paddy soil): A comparative
690 advanced solid state NMR study. Sci. Total Environ. 576, 444–452.
691 https://doi.org/10.1016/j.scitotenv.2016.10.118

692 Yruela, I., 2005. Copper in plants. Brazilian J. Plant Physiol. 17, 145–156.
693 https://doi.org/10.1590/s1677-04202005000100012

694 Yuan, D.H., Guo, X.J., Wen, L., He, L.S., Wang, J.G., Li, J.Q., 2015. Detection of
695 Copper (II) and Cadmium (II) binding to dissolved organic matter from
696 macrophyte decomposition by fluorescence excitation-emission matrix spectra
697 combined with parallel factor analysis. Environ. Pollut. 204, 152–160.
698 https://doi.org/10.1016/j.envpol.2015.04.030

699 Zhu, B., Pennell, S.A., Ryan, D.K., 2014. Characterizing the interaction between uranyl
700 ion and soil fulvic acid using parallel factor analysis and a two-site fluorescence
701 quenching model. Microchem. J. 115, 51–57.
702 https://doi.org/10.1016/j.microc.2014.02.004

703 Zhu, B., Ryan, D.K., 2016. Characterizing the interaction between uranyl ion and fulvic
704 acid using regional integration analysis (RIA) and fluorescence quenching. J.
705 Environ. Radioact. 153, 97–103. https://doi.org/10.1016/j.jenvrad.2015.12.004

706

707